J|A|C|S
ARTICLES
Published on Web 04/07/2007

Ultrafast Proton Transfer to Solvent: Molecularity and Intermediates from Solvation- and Diffusion-Controlled Regimes

J. L. Pérez-Lustres,[†] F. Rodriguez-Prieto,[‡] M. Mosquera,*[,‡] T. A. Senyushkina,[†] N. P. Ernsting,[†] and S. A. Kovalenko*[,†]

Contribution from the Institute for Chemistry, Humboldt University of Berlin, Brook-Taylor-Strasse 2, 12489 Berlin, Germany, and Physical Chemistry Department, Chemistry Faculty, University of Santiago, Avda. Das Ciencias s/n, 15706 Santiago de Compostela, Spain

Received September 8, 2006; E-mail: skovale@chemie.hu-berlin.de; qfmmgfot@usc.es

Abstract: Photoinduced proton transfer (PT) from cations 6-hydroxyquinolinium (6HQc) and 6-hydroxy-1-methylquinolinium (6MQc) to water and alcohols, and solvation of the zwitterionic conjugate base 1-methylquinolinium-6-olate (6MQz) were studied with stationary and transient absorption spectroscopy and by quantum chemical calculations. Transient emission spectra from 6MQz in acetonitrile and protic solvents shift dynamically to the red without changing their shape and intensity. The shift matches the solvation correlation function $C(t)$ either measured with known solvatochromic probes coumarin 343 and coumarin 153 or derived from infrared/dielectric-loss data on neat solvents. This indicates that 6MQz monitors the solvation dynamics and that no intramolecular electron transfer occurs on a subpicosecond or longer time scale. The PT dynamics $S(t)$ from 6HQc and 6MQc closely follows $C(t)$, being initially 2−3 times slower. This allows for the conclusion that PT is controlled by solvation, with a barrier of 2 kJ/mol. In water, a pre-condition of this ultrafast reaction seems to be hydrogen-bonding between the negatively charged oxygen and two water molecules, resulting in a complex 6HQc:H_2O:H_2O. The complex is stable due to a high (47 kJ/mol) bonding energy between 6HQc and a water molecule. In acetonitrile, the reaction equilibrium is strongly shifted to the cation. There an intermediate PT state was detected, which may be ascribed to the cationic form 6HQc:H_2O due to residual water impurities. In water−acetonitrile mixtures, the ultrafast solvent-controlled PT is followed by a diffusion-controlled reaction; the measured rate $k_D \approx 10^{10}$ s^{-1} M^{-1} is characteristic for simple bimolecular diffusion. The dependence of the short-time PT signal on water concentration can be fitted with a Poisson distribution of water molecules around the cation. Altogether, the short-time and long-time behaviors provide strong evidence that diffusion of only one water molecule is sufficient to detach the proton. Subsequent solvent stabilization of the products completes the PT reaction.

1. Introduction

Photoinduced solute−solvent proton transfer (PT) may be viewed as a series of elementary steps occurring on different time scales.[1,2] One can distinguish electronic redistribution upon photoexcitation (subfemtosecond), hydrogen bond rearrangement (femtosecond), proton dissociation followed by proton solvation and zwitterion solvation (subpicosecond to picosecond), and diffusion processes (picosecond to nanosecond).[1] All four stages are also present in bimolecular PT which, however, requires diffusion of the reactants to contact distances. Thus, for barrierless intermolecular PT, diffusion is the limiting step and all other faster processes remain obscure. This limitation can be overcome for PT to solvent, where the reactant is already in contact with solvent molecules. It is only necessary to trigger the reaction of interest. Photoacids, molecules which experience an instantaneous change of acidity upon optical excitation, are very convenient in this sense. Femtosecond optical excitation of the photoacid in proton-accepting solvents unleashes the PT reaction which can be monitored with ultrafast spectroscopy.

6-Hydroxyquinolinium (6HQc) and 6-hydroxy-1-methylquinolinium (6MQc) (see Scheme 1) are well-known strong photoacids exhibiting photoinduced solute−solvent PT in aqueous solution and alcohols.[3−9] Earlier reports[3,4] established, mainly by means of fluorimetric titration, that upon optical excitation the acidity of the compounds greatly increases; their pK_a changes from 7 in the ground electronic state to −4 in the excited state. Accordingly, effective deprotonation of the hydroxyl group takes

[†] Humboldt University of Berlin.
[‡] University of Santiago.

(1) Agmon, N. *J. Phys. Chem. A* **2005**, *109*, 13−35.
(2) Tolbert, L. M.; Solntsev, K. M. *Acc. Chem. Res.* **2002**, *35*, 19−27.
(3) Mason, S. F.; Philip, J.; Smith, B. E. *J. Chem. Soc. A* **1968**, 3051−3056.
(4) Schulman, S.; Fernando, Q. *Tetrahedron* **1968**, *24*, 1777−1783.
(5) (a) Bardez, E.; Chatelain, A.; Larrey, B.; Valeur, B. *J. Phys. Chem.* **1994**, *98*, 2357−2366. (b) Bardez, E.; Fedorov, A.; Berberan-Santos, M. N.; Martinho, J. M. G. *J. Phys. Chem. A* **1999**, *103*, 4131−4136.
(6) Kim, T. G.; Kim, Y.; Jang, D.-J. *J. Phys. Chem. A* **2001**, *105*, 4328−4332.
(7) Poizat, O.; Bardez, E.; Buntinx, G.; Alain, V. *J. Phys. Chem. A* **2004**, *108*, 1873−1880.
(8) Kim, T. G.; Topp, M. R. *J. Phys. Chem. A* **2004**, *108*, 10060−10065.
(9) By "solvation" we mean rearrangement of polar solvent molecules upon an instantaneous change of the solute dipole due to optical excitation. This is also known as nonspecific solvation (or simply solvation), in contrast to specific solvation, for example due to hydrogen-bonding.

10.1021/ja0664990 CCC: $37.00

Scheme 1. Acid−Base Equilibria in the Ground Electronic State of 6-Hydroxyquinolinium (6HQc)[a]

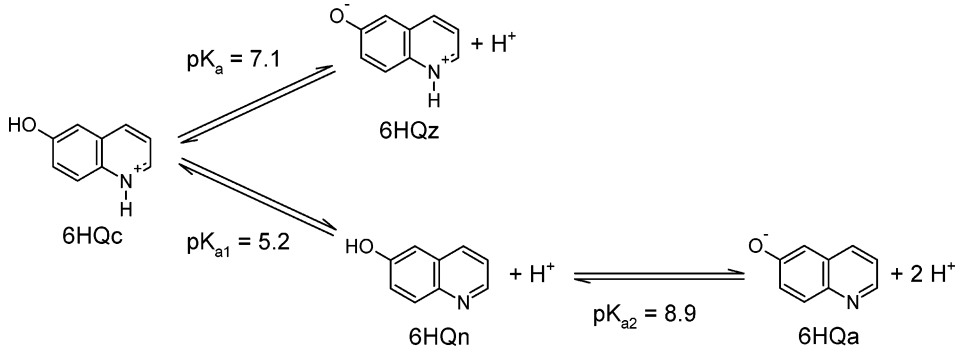

[a] For 6-hydroxy-1-methylquinolinium (6MQc), only the equilibrium between 6MQc and 6MQz has to be considered.

place, resulting in the excited zwitterions, 6HQz and 6MQz, and a proton. Later studies by Bardez et al.[5] confirmed the high acidity of 6HQc, but those authors proposed, on the basis of fluorescence decay measurements, that the PT equilibrium is not established in the excited state even in highly acidic media. It was concluded that no back-reaction occurs even in 10 M perchloric acid solutions.[5a] This unusual behavior was interpreted assuming that PT is coupled to intramolecular electron transfer (ET) from the negatively charged oxygen to the pyridinium ring.[5,7,8] A few transient studies[6−8] published so far on 6HQc and 6MQc dealt with various aspects of the PT dynamics in basic and acidic media. In particular, in acidic aqueous solution the deprotonation time of 2 ps was reported,[7,8] while the intramolecular ET was assumed to occur on a 0.5 ps time scale.[8]

In the present paper we deal mainly with proton dissociation and solvation[9] as well as with diffusion processes. Electronic and H-bond reorganization upon optical excitation remain unresolved. We point out the role of the H-bonding between the OH group of the cation and neighboring water molecules.[10,11] This bonding is initially established in the ground electronic state, resulting in a complex 6HQc:H_2O:H_2O or 6MQc:H_2O:H_2O, and appears to be a necessary condition for the observed ultrafast reaction. For pure solvents (water and alcohols) we demonstrate the key role of the solvation coordinate $C(t)$. Being slower than other processes, $C(t)$ determines the PT rate. A theoretical approach for this type of reactions has been already developed[12,13] and will be used in our analysis. It is worth noting that recent experimental studies[13−18] give indications of the solvent-controlled PT processes. Our work on the above strong photoacids continues this line of research.

We apply the broadband pump−supercontinuum probe technique[19−23] to monitor transient absorption spectra in the range 270−690 nm with 50 fs resolution. Note, in the present case, both the solvation and PT dynamics can be independently measured with two very similar probes, 6MQz and 6MQc. Moreover, 6MQz is the successor of 6MQc in the reaction of interest. It is therefore quite natural to start with measurements on 6MQz.[23] These provide us with solvation correlation functions $C(t)$ which can then be compared to PT kinetics $S(t)$ from 6MQc and 6HQc in the same set of solvents. This comparison shows that solvation is the true reaction coordinate which controls the PT rate. A new feature appearing in acetonitrile and acetonitrile−water mixtures is that the PT signal consists of two distinct contributions: a short-time solvation-controlled component and a diffusion component on a longer time scale. The analysis of these contributions allows one to conclude that diffusion of only *one water molecule* to the primarily formed complex 6HQc:H_2O is sufficient to initiate PT. Subsequent solvent relaxation stabilizes the products and completes the PT reaction.

2. Experimental Section

6-Hydroxyquinoline and 6-methoxyquinoline were purchased from Aldrich and used without further purification. 6-Hydroxy-1-methylquinolinium perchlorate was prepared from 6-hydroxyquinoline as described elsewhere.[23] 6-Hydroxyquinolinium was prepared from 6-hydroxyquinoline solutions by shifting the ground-state acid−base equilibrium toward the acidic form at pH ∼3, with [$HClO_4$] ≈ 10^{-3} M. Solutions were freshly prepared in spectroscopic-grade solvents (Aldrich and Merck) and double-distilled water. pH was controlled with $HClO_4$, NaOH, and self-made acetic acid/sodium acetate and sodium hydrogen phosphate/sodium dihydrogen phosphate buffers (all reactants Merck p.a.). pH was measured with a Radiometer PHM-82 pH-meter equipped with a radiometer Type B combined electrode.

Absorption spectra were scanned with a Varian Cary 3E spectrometer. Fluorescence excitation and emission spectra were recorded with a Spex Fluorolog-2 spectrofluorimeter and corrected for instrument factors. Fluorescence quantum yields Φ were measured by using quinine sulfate in aqueous H_2SO_4 (0.5 M) as standard (Φ = 0.546).[24]

(10) Solntsev, K. M.; Clower, C. E.; Tolbert, L. M.; Huppert, D. *J. Am. Chem. Soc.* **2005**, *127*, 8534−8544.
(11) Pines, E.; Pines, D. In *Ultrafast hydrogen bonding dynamics and proton transfer processes in the condensed phase*; Elsaesser, T., Bakker, H. J., Eds.; Kluwer Academic Publishers: Dordrecht, The Netherlands, 2002; pp 155−184.
(12) Kiefer, P. M.; Hynes, J. T. *Solid State Ionics* **2004**, *168*, 219−224.
(13) Hynes, J. T.; Tran-Thi, T.-H.; Granucci, G. *J. Photochem. Photobiol. A* **2002**, *154*, 3−11.
(14) (a) Cohen, B.; Segal, J.; Huppert, D. *J. Phys. Chem. A* **2002**, *106*, 7462−7467. (b) Cohen, B.; Leiderman, P.; Huppert, D. *J. Phys. Chem. A* **2002**, *106*, 11115−11122.
(15) Tran-Thi, T.-H.; Gustavsson, T.; Payer, C.; Pommeret, S.; Hynes, J. T. *Chem. Phys. Lett.* **2000**, *329*, 421−430.
(16) Rini, M.; Pines, D.; Magnes, B.-Z.; Pines, E.; Nibbering, E. T. J. *J. Chem. Phys.* **2004**, *121*, 9593−9610.
(17) Leiderman, P.; Genosar, L.; Huppert, D. *J. Phys. Chem. A* **2005**, *109*, 5965−5977.
(18) Peon, J.; Polshakov. D.; Kohler, B. *J. Am. Chem. Soc.* **2002**, *124*, 6428−6438.
(19) Kovalenko, S. A.; Dobryakov, A. L.; Ruthmann, J.; Ernsting, N. P. *Phys. Rev. A* **1999**, *59*, 2369−2381.
(20) Kovalenko, S. A.; Schanz, R.; Hennig, H.; Ernsting, N. P. *J. Chem. Phys.* **2001**, *115*, 3256−3272.
(21) Kovalenko, S. A.; Lustres, J. L. P.; Ernsting, N. P.; Rettig. W. *J. Phys. Chem. A* **2003**, *107*, 10228−10232.
(22) Ruthmann, J.; Kovalenko, S. A.; Ernsting, N. P.; Ouw, D. *J. Chem. Phys.* **1998**, *109*, 5466−5468.
(23) Lustres, J. L. P.; Kovalenko, S. A.; Mosquera, M.; Senyushkina, T.; Flasche, W.; Ernsting, N. P. *Angew. Chem., Int. Ed.* **2005**, *44*, 2−6.

Fluorescence lifetimes were determined by single-photon counting (0.2 ns resolution) with a CD-900 spectrometer from Edinburgh Instruments. All measurements were done at 298 K.

Femtosecond transient absorption was measured with the pump−supercontinuum probe (PSCP) technique.[19−23] Briefly, an optical parametric amplifier (TOPAS, Light Conversion) pumped by a Ti:Sa laser (Femtolasers) delivered ~2 μJ, 50 fs, 90 Hz pulses at 430 or 360 nm to excite 6MQz or 6MQc and 6HQc, respectively. The second harmonic (400 nm) of the fundamental was focused in 1 mm CaF_2 to generate the supercontinuum probe in the range 270−690 nm. The pump and probe were focused in a 0.2 mm spot on the sample flowing in an optical cell of 0.4 mm thickness. The absorbance A was about 0.8, corresponding to a sample concentration 5×10^{-3} M. The probe signal was spectrally dispersed and registered with a photodiode array (512 pixels). The pump−probe cross-correlation was well below 100 fs over the whole spectrum. The experimental transient spectra $\Delta A(\lambda,t)$ were corrected for the chirp of the supercontinuum and for the solvent contribution.[19] The spectra were recorded with 3, 10, 50, and 200 fs steps, with parallel and perpendicular pump−probe polarization. To improve the signal-to-noise ratio, the data were averaged over multiple pump−probe scans (3−6 scans with 50 shots per temporal point).

Semiempirical calculations were carried out with a development version of VAMP 7.0a.[25] Gas-phase *ab initio* and DFT calculations were carried out with Gaussian 94,[26] revisions E.2 and B.2, running on DEC AS1200 and Fujitsu VPP300 computers.

3. Results and Discussion

3.1. Molecular Properties. Ground- and excited-state molecular properties of the zwitterionic and cationic forms of 6-hydroxyquinoline were characterized by optical spectroscopy and quantum chemical calculations. Note that the cationic form shows two minima for the planar rotameric isomers of the hydroxy group, which are practically isoenergetic. The differences between them are small and are neglected in the following.

A pK_a value of 7.1 for 6MQc was measured by spectrophotometric titration. This value corresponds to deprotonation at the hydroxyl group. By means of the Förster cycle, we estimate that the pK_a* decreases to −4 in the S_1 excited state. For 6HQc, the first deprotonation occurs at the N position and has pK_{a1} = 5.2 (see Scheme 1). 6-Methoxyquinoline shows the same pK_a. The deprotonation at the hydroxyl group of 6HQ shows pK_{a2} = 8.9.[3] Note that pK_{a1} and pK_{a2} correspond to the microscopic equilibria involving the neutral non-zwitterionic form, 6HQn, in Scheme 1. For 6HQ, the tautomeric equilibrium between the neutral and zwitterionic forms is completely shifted toward the former.

Cationic and zwitterionic geometries were optimized and characterized as minima of the ground potential energy surface by harmonic frequency analysis at the B3LYP/6-31+G* level of theory.[26] The molecule is polarized along the axis drawn by the two most electronegative atoms: N and O. Ground-state dipole moments are 4 and 10 D for the cation and zwitterion, respectively, according to the DFT calculations in the gas phase. For the cationic form, the dipole moment is referred to the center of mass. It is estimated, by means of semiempirical AM1-PECI[25] calculations (76 configurations), that the dipole moment of 6MQz decreases by 4−5 D upon excitation to S_1. The decrease of the dipole moment is consistent with the negative solvatochromism observed in alcohols and water. Other solvents could not be investigated due to the low solubility of 6MQz. The magnitude of the solvatochromic shifts measured in water and methanol agrees with a decrease of the dipole moment by 4−5 D for a spherical molecular cavity with radius a = 3.35 Å and an isotropic polarizability α = 20 Å^3.[23]

Since PT may be strongly enhanced by solute−solvent hydrogen-bonding, it is necessary to explore the stability of the complex 6MQc:H_2O. This was done with quantum chemical calculations at the B3LYP/6-31+G* level. The linear conformation was optimized and characterized as the minimum by harmonic frequency analysis at the same level. After correcting for zero-point energies and the basis set superposition error, we get a stabilization energy of 47 kJ/mol, which is 4 times higher than the H-bonding in neat water. Therefore, 6MQc should be present in water predominantly in the form 6MQc:H_2O (so-called preferential solvation[27]). This should also be true for acetonitrile because of residual water impurities.

The structure of 6MQc:H_2O exhibits C_s symmetry, and the water molecule is perpendicular to the symmetry plane, which contains the 6MQc molecule. The hydrogen bond is established between the water O and the hydroxyl proton. Characteristic parameters are a O···O distance of 2.74 Å, a H···O distance of 1.75 Å, and nonlinearity α of 0.3° (angle subtended by the hydroxyl O−H bond line and the O···O line). The plane of the water molecule forms an angle β of 138° with the O···O line. Remarkably, the O···O and H···O distances are significantly shorter than in the 6-hydroxyquinoline:H_2O (6HQn:H_2O)[28] and 3-methoxyphenol:H_2O (3MP:H_2O)[29] complexes, which also show smaller stabilization energies. In 6HQn:H_2O the O···O distance is 2.90 Å, whereas the H···O distance is 1.95 Å and the stabilization energy amounts to 25 kJ/mol, according to RHF/6-31G** calculations. A H···O distance of 1.81 Å and a stabilization-energy 27 kJ/mol are estimated for the 3MP:H_2O adduct at the B3LYP/cc-pVDZ level of theory.

3.2. Stationary Spectra and Lifetimes. Figure 1 shows normalized stationary absorption $\sigma_A(\lambda)$ and stimulated emission $\sigma_E(\lambda)$ spectra of 6MQc and of 6MQz in water and acetonitrile. The stationary spectra in alcohols (not shown) are similar to those in water. Note that the stimulated emission line shapes $\sigma_E(\lambda) = \lambda^4 F(\lambda)$ are calculated from the originally measured fluorescence spectra $F(\lambda)$ by multiplying $F(\lambda)$ by λ^4. In this way, both σ_A and σ_E are given in the same units of cross-sections (or extinction), which is necessary for correct comparison between the two and to transient absorption spectra.[30] Multiplication by λ^4 results in a red-shift and broadening; for example, for 6MQc in water, $\sigma_E(\lambda)$ peaks at 613 nm while $F(\lambda)$ has a maximum at 585 nm.

(24) Melhuish, W. *J. Phys. Chem.* **1961**, *65*, 229.
(25) Clark, T.; Alex, A.; Beck, B.; Chandrasekhar, J.; Gedeck, P.; Horn, A.; Hutter, M.; Martin, B.; Rauhut, G.; Sauer, W.; Schindler, T.; Steinke, T.: *VAMP*, version 7.0a; Oxford Molecular Ltd.: Erlangen, Germany, 1998.
(26) Frisch, M. J.; et al. *Gaussian 94*, Revisions E.2 and B.2; Gaussian, Inc.: Pittsburgh, PA, 1995.
(27) (a) Solntsev, K. M.; Huppert, D.; Agmon, N. *J. Phys. Chem. A* **1998**, *102*, 9599−9606. (b) Solntsev, K. M.; Huppert, D.; Agmon, N. *J. Phys. Chem. A* **1999**, *103*, 6984−6997.
(28) Bach, A.; Hewel, J.; Leutwyler, S. *J. Phys. Chem. A* **1998**, *102*, 10476.
(29) Geppert, W. D.; Ullrich, S.; Dessent, C. E. H.; Müler-Dethlefs, K. *J. Phys. Chem. A* **2000**, *104*, 11870.
(30) In the literature, including textbooks, it is common to compare absorption and fluorescence line shapes. This is not correct, because the two have different dimensions. *Absorption*, $A(\lambda)$, is measured in units of extinction $\epsilon_A(\lambda)$ or cross-section $\sigma_A(\lambda)$, while *fluorescence*, $F(\lambda)$, represents the rate of *spontaneous* emission per unit spectral interval. The correct counterpart of absorption is *stimulated emission*, $\sigma_E(\lambda) = \lambda^4 F(\lambda)$. Here, λ^2 factor comes from the conversion $F(\lambda) \rightarrow F(\nu)$, and another λ^2 originates from the relationship between spontaneous and stimulated emission rates. See: Birks, J. B. *Photophysics of aromatic molecules*; Wiley-Interscience: New York, 1970; Sections 3 and 4, in particular Figure 4.2.

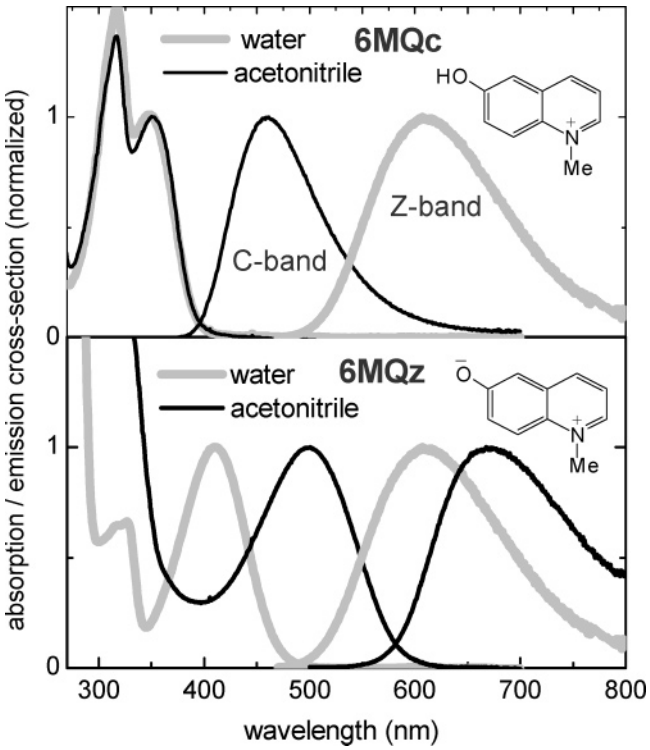

Figure 1. Stationary absorption and stimulated emission spectra of 6-hydroxy-1-methylquinolinium (cation 6MQc, top) and of 1-methylquinolinium-6-olate (zwitterion 6MQz, bottom) in water (gray) and acetonitrile (black). In acetonitrile 6MQc emits about 450 nm (C-band), while in water emission comes from the zwitterion (Z-band) due to photoinduced PT. Measured fluorescence spectra are multiplied by λ^4 to obtain the stimulated emission line shapes. In this way, both absorption and emission are given in the same units of normalized cross-section (or extinction), allowing for correct comparison between the two and to transient absorption spectra.

The absorption spectra of 6MQ in acidic water and acetonitrile ($[HClO_4] = 10^{-4}$ M; Figure 1, top) are nearly indistinguishable, with absorption maxima at 315 and 350 nm. The ground-state acid−base equilibrium is completely shifted toward the cationic form 6MQc in these conditions.[3,4] However, this is not the case in the excited state. In water the emission spectrum is strongly red-shifted relative to absorption and shows the same shape and position as the emission from the zwitterion 6MQz (Z-band). Fluorescence in water shows an ~1 ns lifetime and quantum yield $\Phi = 0.01$. The excitation spectrum measured about 600 nm reproduces the absorption spectrum of the cation. Therefore, PT to solvent in the excited state has to be concluded.[4] On the other hand, in acetonitrile emission peaks at 460 nm and decays in 28 ns and $\Phi = 0.3$. The fluorescence band and the decay time of 6MQc are nearly indistinguishable from those of 6-methoxyquinolinium, demonstrating that emission in acetonitrile originates from the excited cation (C-band). From this analysis, one expects that early transient absorption spectra in acidic water will show the locally excited cation emission around 460 nm (C-band, similar to emission in acetonitrile), which should decay with time. Simultaneously, the zwitterionic Z-band at 613 nm is expected to grow up.

The spectra of 6MQz in water (both absorption and emission) are blue-shifted relative to those in acetonitrile (Figure 1, bottom). This negative solvatochromism is due to the above-mentioned decrease of the molecular dipole moment by 4−5 D upon photoexcitation. The Stokes shift between the absorption and emission spectra in water, about 8000 cm^{-1}, consists of intramolecular $\Delta\nu_{intra}$ and solvent $\Delta\nu_{solv}$ reorganization. We demonstrated in a previous paper[23] that the intramolecular part is due to optically active high-frequency vibrational modes and is too fast to be resolved in our femtosecond pump−probe measurements. At the same time, solvent relaxation occurring on a subpicosecond to picosecond time scale can be well measured with the present technique. The shift $\Delta\nu_{solv}$ can be estimated as[3131]

$$\Delta\nu_{solv} = f(\epsilon,n)\frac{(\mu_1 - \mu_2)^2}{a^3} \approx 3000\ \text{cm}^{-1} \qquad (1)$$

where $f(\epsilon,n) = 2(\epsilon - 1)/(2\epsilon + 1) - 2(n - 1)/(2n + 1)$ is the reaction field factor, with ϵ and n being solvent susceptibility and refractive index, respectively, and $a = 3.35$ Å is the cavity radius. Accordingly, in time-resolved measurements, one expects to monitor a transient emission red-shift on the time scale of solvent relaxation, similar to that observed with other solvatochromic probes such as coumarin 153 (C153),[31] coumarin 343 (C343),[32] and aminonitrofluorene.[22]

3.3. Transient Spectroscopy of 6MQz. Transient absorption spectra of 6MQz in water upon excitation at 430 nm are displayed in Figure 2. Recall that the differential signal $\Delta A(\lambda,t)$ consists of three contributions: excited-state absorption (ESA), bleach, and stimulated emission (SE). ESA enters with a positive sign, while SE and bleach are negative.[18−23] The pump−probe delays from 0.06 to 2 ps are indicated. The signal is dominated by ESA in the blue (λ < 370 nm) and by bleach and SE in the red (λ > 400 nm). The bleach band corresponds to negative absorption and peaks at 410 nm, as expected from the stationary spectrum on top. Similarly, the SE band at 2 ps peaks about 615 nm, close to the emission maximum. The spectral evolution occurs mainly in the red region and can be well described as a transient Stokes shift of the SE band. Using the fact that the evolution of ESA and bleach is apparently weak, one can decompose the transient spectra to isolate the evolving SE contribution. This decomposition is shown in Figure 2c. The SE band moves from 535 to 615 nm; the full shift of 2500 cm^{-1} is in agreement with the estimate (1). Note that the earliest spectrum at 0.06 ps is red-shifted relative to absorption by ~5000 cm^{-1}. This "instantaneous" (unresolved in our experiment) contribution should be ascribed to intramolecular reorganization on a 10 fs time scale.[31]

The transient SE spectra can be fitted with log-normals to calculate the spectral relaxation function,

$$C(t) = (\nu^m(t) - \nu_\infty^m)/(\nu_0^m - \nu_\infty^m) \qquad (2)$$

where $\nu^m(t)$ is the time-dependent peak frequency of the SE band, and ν_0^m and ν_∞^m are measured at zero and infinite delays. The resulting $C(t)$ values are shown in Figure 3 for 6MQz (gray curves) and for C153 (black).[33] Note an excellent agreement

(31) (a) Horng, M. L.; Gardecki, J. A.; Papazyan, A.; Maroncelli, M. *J. Phys. Chem.* **1995**, *99*, 17311−17337. (b) Reynolds, L.; Gardecki Frankland, S. J. V.; Horng, M. L.; Maroncelli, M. *J. Phys. Chem.* **1996**, *100*, 10337−10354.

(32) Jimenez, R.; Fleming, G. R.; Kumar, P. V.; Maroncelli, M. *Nature* **1994**, *369*, 471−474.

(33) These measurements were done with the same experimental conditions (the same excitation at 430 nm and the probe continuum), except that the sample was C153 instead 6MQz. A full account will be given elsewhere: Senyushkina, T. A.; Kovalenko, S. A.; Ernsting N. P. Solvation dynamics of coumarin 153 from transient absorption spectroscopy, manuscript in preparation.

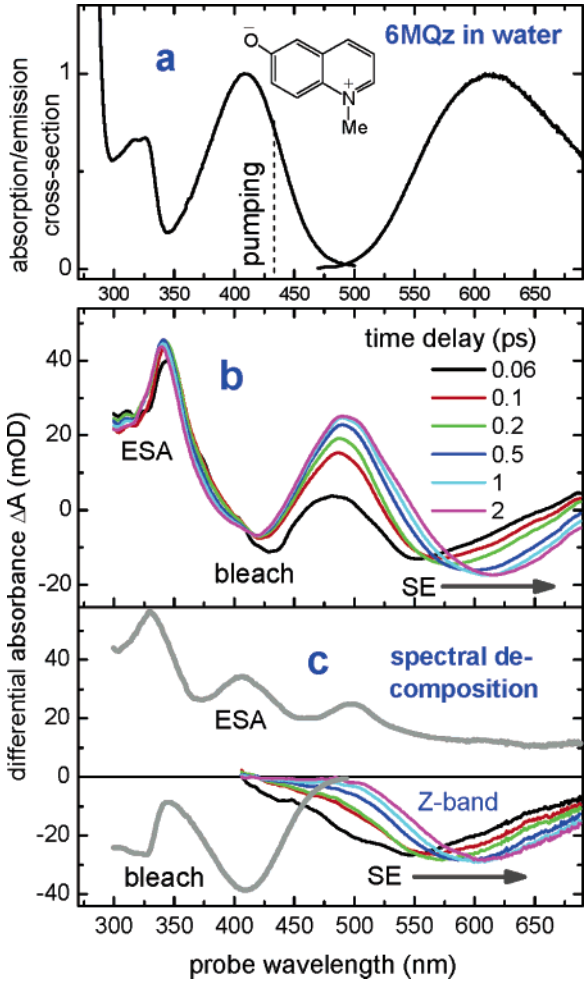

Figure 2. (a) Stationary spectra of 6MQz in water. Femtosecond excitation at 430 nm is marked by a dashed line. (b) Transient absorption spectra $\Delta A(\lambda,t)$ from 0.06 to 2 ps, monitoring solvation of 6MQz, seen as a continuous Stokes shift of stimulated emission (SE) to the red, as indicated by the arrow. (c) Decomposition of the transient spectra in SE, bleach, and excited-state absorption (ESA). In this decomposition, ESA and bleach experience no evolution.

between the values for the two probes from our measurements and the literature data (dashed curves). Furthermore, we have shown elsewhere[23] that our results for 6MQz in water and methanol are consistent with the solvent fluctuation correlation functions derived from IR/dielectric-loss data on neat solvents. Therefore, 6MQz monitors solvation dynamics similar to other solvatochromic probes like coumarins[31−34] or aminonitrofluorene,[22] and no intramolecular ET occurs in the phoptoexcited 6MQz on a subpicosecond or longer time scale. Indeed, the evolution after 0.06 ps is nicely described by the solvent relaxation, so no place remains for other processes such as intramolecular ET.

The measured solvent relaxation functions $C(t)$ were fitted empirically with three exponentials or with a Gaussian and two exponentials:

$$C(t) = a_1 \exp(-t^2/2\tau_1^2) + a_2 \exp(-t/\tau_2) + a_3 \exp(-t/\tau_3) \quad (3a)$$

$$\tau_0^{-1} = \sum a_j \tau_j^{-1}, \quad \langle\tau\rangle = \sum a_j \tau_j \quad (3b)$$

where τ_j and a_j are the time constants and amplitudes, and the parameters τ_0 and $\langle\tau\rangle$ characterize the short-time and long-time behaviors. The fit parameters are collected in Table 1. By comparing the fits for 6MQz and C153, a good agreement is found on a long time scale (τ_3, a_3, and $\langle\tau\rangle$) for all solvents except 1-propanol. At short times (τ_1, τ_2, and τ_0) the agreement is still good for acetonitrile, but in other solvents there are deviations between 6MQz and C153. It follows that the short time constants are determined with an accuracy of factor of 2.

3.4. Proton Transfer from 6MQc and 6HQc. Transient spectra from the two cations in water are shown in Figure 4 for pump−probe delays of 0.1, 0.2, 0.5, 1, 2, and 5 ps. The evolution is quite similar for both probes. At early times, SE peaks at 450 nm, exactly at the position of the C-band. With increasing time, the C-band decays and the Z-band at 615 nm develops. This evolution corresponds to solute−solvent PT, as discussed in section 3.2. The transient spectra can be decomposed in various contributions, similar to those of the zwitterion. Such decomposition for 6MQc in water is presented in Figure 5. Here bleach (blue), ESA (cyan), cation emission (green), and zwitterions emission (magenta) are shown together with the original spectra (thin black). The C-band and Z-band are close in magnitude, and therefore the same is true for the corresponding cross-sections. The transient ESA spectra experience a small change mainly in the blue region (λ < 450 nm), while in the red the evolution is well described by decay and rise of the C-band and Z-band, respectively. At early time (0.1 ps), the Z-band is very weak and peaks at 550−570 nm. With increasing time the band rises in magnitude and shifts to the red, approaching the stationary spectrum between 2 and 5 ps. This red-shift, by analogy with Figure 2, should be assigned to solvation of the zwitterion occurring in the course of the PT reaction.

A quantitative description of the PT dynamics is obtained with the help of suitably chosen band integrals,[20]

$$\mathrm{BI}(\lambda_1,\lambda_2) = \int_{\lambda_1}^{\lambda_2} \Delta A(t,\lambda)\, \mathrm{d}\lambda/\lambda \quad (4)$$

which represent the time-dependent signal averaged over the C-band or Z-band. For example, for the C-band, one calculates BI(417,525) between the quasi-isosbestic points λ_1 = 417 nm and λ_2 = 525 nm (see Figure 4), and similarly BI(525,689) for the Z-band. The behavior of these integrals for 6MQc (gray lines) and 6HQc (thin black) is shown in Figure 6a. The curves for the two cations are indistinguishable except for an offset. Therefore, in the rest of this paper we consider the PT dynamics from 6HQc only. Figure 6b shows the same but normalized integrals $S(t)$ for the C-band (dashed) and for the Z-band (solid), together with their average (gray). As expected, the two bands show very similar evolution, except that the Z-band rises slightly faster than the C-band decays. This discrepancy is due to a spectral cutoff. Since the Z-band shifts to the red, a part of the signal goes out of the detection window, resulting in an accelerated decay. The difference is, however, small, and we neglect this effect in the following.

The functions $S(t)$ were fitted with three exponentials, and the results for both $S(t)$ and $C(t)$ are collected in Table 2,

(34) Gustavsson, T.; Cassara, L.; Gulbinas, V.; Gurzadyan, G.; Mialocq, J.-C.; Pommeret, S.; Sorgius, M.; van der Meulen, P. *J. Phys. Chem. A* **1998**, *102*, 4229−4245.

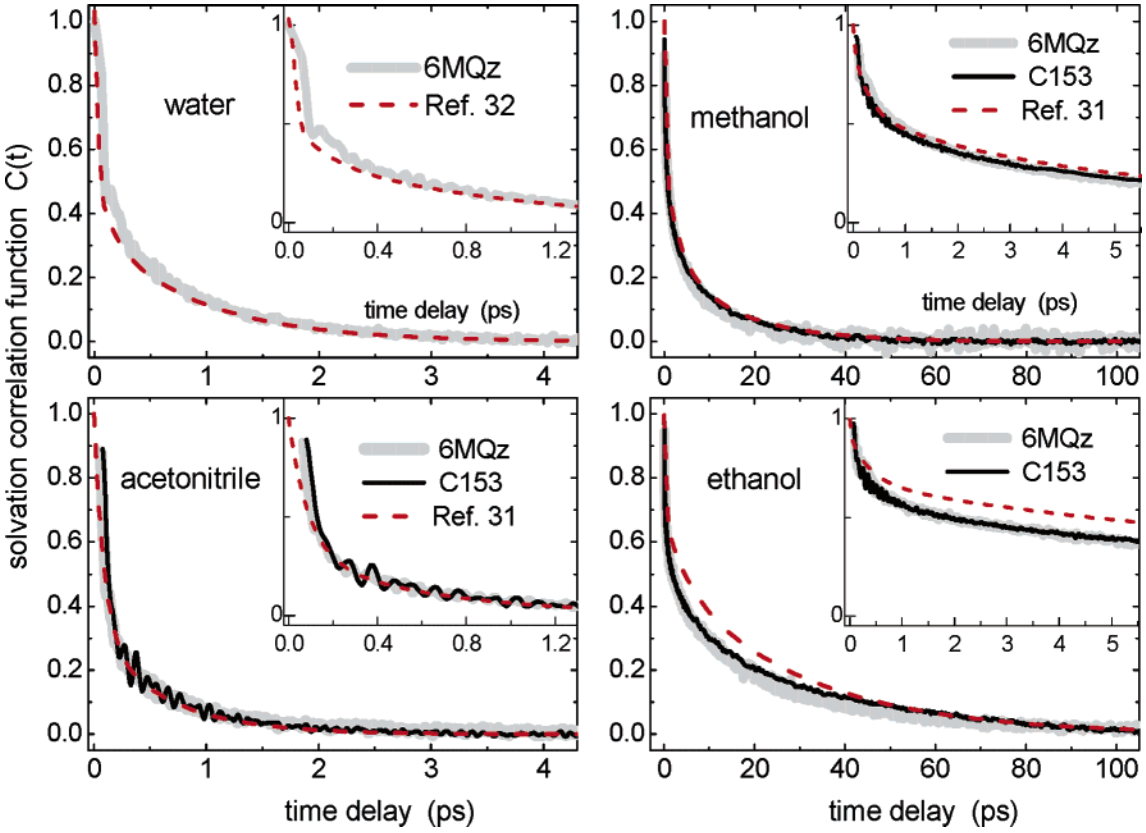

Figure 3. Solvation dynamics of 6MQz (gray curves) and of coumarin 153 (C153, black) in water, acetonitrile, methanol, and ethanol. Dashed red lines reproduce the literature data.[31,32] The solvation correlation functions $C(t) = (\nu^m(t) - \nu_\infty^m)/(\nu_0^m - \nu_\infty^m)$ are derived from transient spectra, such as in Figure 2. $\nu^m(t)$ is the time-dependent peak frequency of the SE band, with ν_∞^m and ν_0^m taken at infinite and zero delays. Fits of $C(t)$ are collected in Table 1.

Table 1. Solvation Dynamics $C(t)$ from 6MQz, C153, and C343[a]

solvent	probe	ν_0^m (cm^{-1})	ν_∞^m (cm^{-1})	a_1	τ_1 (ps)	a_2	τ_2 (ps)	a_3	τ_3 (ps)	τ_0 (ps)	$\langle\tau\rangle$ (ps)
H_2O	6MQz	18 700	16 330	0.39[G]	0.049	0.29	0.24	0.32	1.0	0.11	0.42
	C343[32]	22 222	20 269	0.48[G]	0.026	0.20	0.13	0.35	0.9	0.05	0.35
	6MQz	17 070	14 790	0.75	0.070	0.25	0.66	-	-	0.09	0.22
MeCN	C153	20 435	18 600	0.65[G]	0.075	0.35	0.63	-	-	0.11	0.27
	C153[31]			0.69	0.089	0.31	0.63	-	-	0.12	0.26
′	6MQz	17 800	15 370	0.31[G]	0.11	0.39	1.61	0.30	11	0.32	4.0
MeOH	C153	20 210	17 890	0.30[G]	0.11	0.36	0.98	0.34	12	0.32	4.5
	C153[31]			0.34	0.28	0.30	3.2	0.26	15	0.21	5.0
				0.10	0.03						
	6MQz	17 290	15 300	0.29	0.11	0.31	2.7	0.40	26	0.36	11
EtOH	C153	20 330	18 120	0.27[G]	0.12	0.23	1.7	0.50	27	0.42	14
	C153[33]			0.23	0.39	0.18	5.0	0.50	30	0.29	16
				0.09	0.03						
	6MQz			0.36	0.31	0.27	4.3	0.37	26	0.81	11
PrOH	C153	20 290	18 270	0.24[G]	0.13	0.25	3.2	0.51	49	0.52	26
	C153[33]			0.17	0.34	0.23	6.6	0.51	48	0.29	26
				0.09	0.03						

[a] Fit parameters of the solvation correlation functions $C(t)$ shown in Figure 3. The fits $C(t) = \sum a_j \exp(-t/\tau_j)$ are two- or three-exponential or the first component $a_1 \exp(-t^2/2\tau_1^2)$ is a Gaussian (marked with superscript G). ν_0^m and ν_∞^m are band peaks of the time-zero and stationary SE spectra. $\tau_0^{-1} = \sum a_j \tau_j^{-1}$ is the averaged decay rate, and $\langle\tau\rangle = \sum a_j \tau_j$ is the average decay time. The second line for each solvent reproduces the literature data (from ref 31 or 32, as indicated; red dashed curves in Figure 3) in which the fits for methanol, ethanol, and propanol are four-exponential (their first and second components are displayed in the same columns (a_1, τ_1)).

allowing for comparison between the PT and solvation dynamics. One can also compare $S(t)$ to $C(t)$ directly by plotting these functions together, as shown in Figure 7. Here $C(t)$ (gray) was measured with 6MQz for water, methanol, and ethanol and with C153 for 1-propanol and 1-butanol. The left and right columns display these functions on long and short time scales, respectively. The main feature evident from Figure 7 is that the PT dynamics closely follows the solvation dynamics. This indicates strongly that PT is solvation-controlled. In other words, Figure 7 tells us that $C(t)$ is the true reaction coordinate[12,13,35] and that other processes, such as intrinsic PT, must be much faster than solvation, hence taking place on a 10 fs or shorter time scale.

(35) Van der Zwan, G.; Hynes, J. T. *J. Phys. Chem.* **1985**, *89*, 4181−4188.

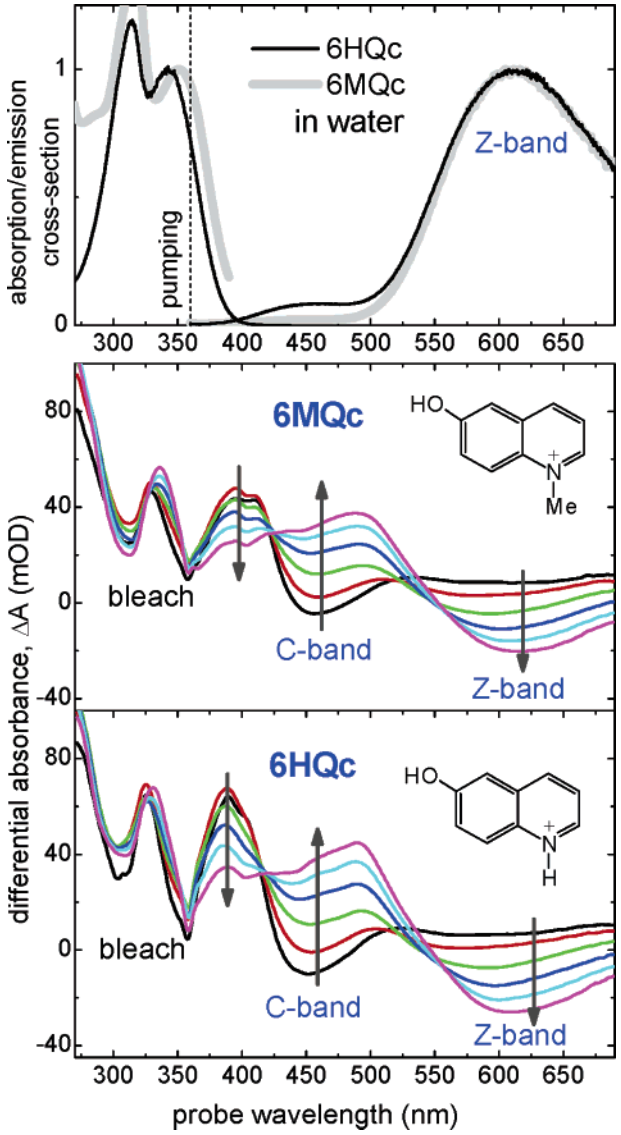

Figure 4. Proton transfer (PT) from 6MQc and 6HQc to water after excitation at 360 nm. Stationary stimulated emission spectra (top) show the PT band (Z-band) at 615 nm. Transient spectra are displayed for pump−probe delays: 0.1 (black), 0.2 (red), 0.5 (green), 1 (blue), 2 (cyan), and 5 ps (magenta). PT is recognized from the decay of the C-band at 450 nm and from the concomitant growth of the Z-band at 615 nm, as indicated by arrows.

In this case, a quasi-equilibrium between the reactant and product is "instantaneously" established for any particular solvent configuration. This equilibrium then shifts to the product in the course of "slow" solvent relaxation. It is this shift of the PT quasi-equilibrium that one observes in the spectral evolution in Figure 4.

Transition state theory can be applied along the classical solvent coordinate to estimate the reaction rate,[12]

$$k = 1/\tau_S \exp(-\Delta G^{\ddagger}/k_B T) \qquad (5)$$

where τ_s is a characteristic solvation time, $\Delta G^{\ddagger}$ the reaction barrier, k_B the Boltzmann constant, and T temperature. Strictly speaking, eq 5 is correct only for a monoexponential solvent relaxation. For zero barrier $\Delta G^{\ddagger} = 0$, then, the PT reaction proceeds with the maximal rate $1/\tau_s$ (definition of solvation control). In our case the barrier is nonzero but low, $\Delta G^{\ddagger} \sim k_B T$.

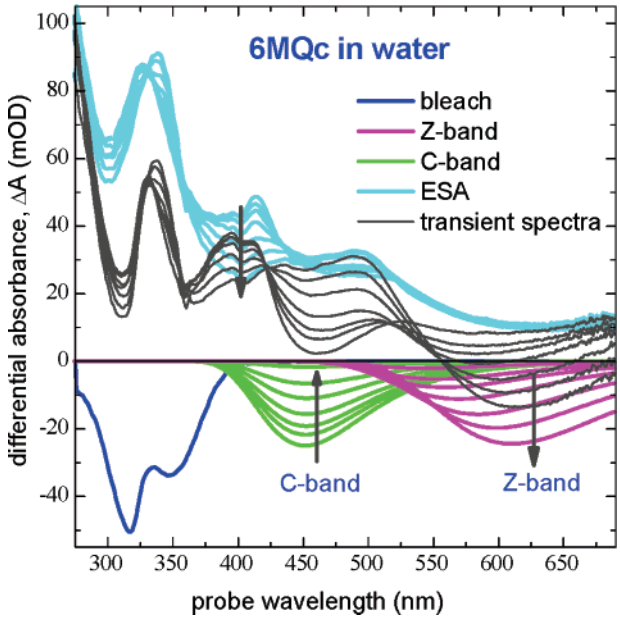

Figure 5. Decomposition of the transient spectra (black) from 6MQc in water (see Figure 4) in bleach (blue), ESA (cyan), and SE, which consists of the decaying C-band (green) and developing Z-band (magenta). Pump−probe delays of 0.1, 0.2, 0.5, 1, 2, and 5 ps are the same as in Figure 4.

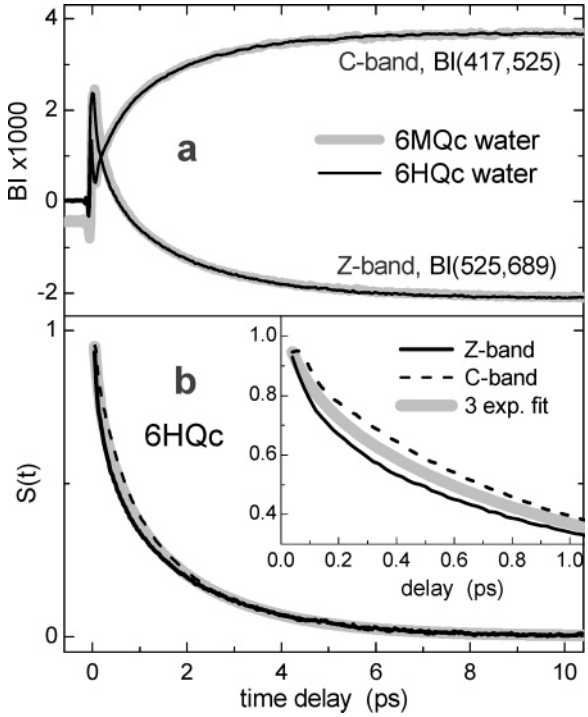

Figure 6. Dynamics of PT from 6MQc (gray) and 6HQc (thin black) to water from band integrals $BI(\lambda_1,\lambda_2) = \int_{\lambda 1}^{\lambda 2} \Delta A(t,\lambda)\, d\lambda/\lambda$: BI(417,525) for the C-band and BI(525,689) for the Z-band. The curves for the two probes are indistinguishable, except for an offset which is due to a different contribution from ESA. (b) The same *normalized* band integrals $S(t)$ for 6HQc together with a fit (gray) for the average over the C-band and Z-band.

As can be seen from Table 2 for water and methanol, the PT characteristic times τ_j are longer by roughly a factor of 2 than those for solvation, resulting in $\Delta G^{\ddagger} \approx 2$ kJ/mol. Interestingly, for ethanol, propanol, and butanol, the short-time τ_0 for PT is still 2−3 times slower than that for solvation, but the long-time $\langle\tau\rangle$ is, in contrast, faster. A qualitative explanation is that the short-time solvent reorganization (given by the amplitudes

Table 2. Comparison of the PT Dynamics $S(t)$ to Solvation Dynamics $C(t)$[a]

solvent	probe	a_1	τ_1 (ps)	a_2	τ_2 (ps)	a_3	τ_3 (ps)	τ_0 (ps)	$\langle\tau\rangle$ (ps)
H_2O	MQz $C(t)$	0.39[G]	0.049[G]	0.29	0.24	0.32	1.0	0.11	0.42
	HQc $S(t)$	0.21	0.071	0.29	0.42	0.50	2.0	0.26	1.14
MeCN	MQz $C(t)$	0.75	0.070	0.25	0.66			0.09	0.22
	HQc $S(t)$	0.72	0.18	0.28	1.21			0.24	0.47
MeOH	MQz $C(t)$	0.31[G]	0.11	0.39	1.6	0.30	11	0.32	4.0
	HQc $S(t)$	0.29	0.34	0.37	2.1	0.34	18	0.95	7.0
EtOH	MQz $C(t)$	0.29	0.11	0.31	2.7	0.40	26	0.36	11
	HQc $S(t)$	0.23	0.45	0.30	3.8	0.47	19	1.6	10
PrOH	C153 $C(t)$	0.24[G]	0.13[G]	0.25	3.2	0.51	49	0.51	26
	HQc $S(t)$	0.21	0.40	0.25	4.3	0.54	31	1.7	18
BuOH	C153 $C(t)$	0.22[G]	0.13[G]	0.24	6.6	0.54	71	0.58	40
	HQc $S(t)$	0.20	0.58	0.32	8.7	0.48	49	2.6	26

[a] The fits $S(t) = \sum a_j \exp(-t/\tau_j)$ are three-exponential with parameters defined as in Table 1.

a_1 and a_2 in Table 1) may be sufficient to complete the PT reaction, and therefore the long-time components (a_3, τ_3) of solvent relaxation have simply no time to contribute. Similar effects have been previously discussed in solvation-controlled intramolecular ET.[36] Since in both cases the theoretical approach is very much the same, the results obtained for ET can be directly applicable for solvation-controlled PT. In particular, a negligible rate of back-PT, $k_{back} = k^0_{back} \exp(-\Delta G^{\ddagger}_{back}/k_B T)$, is naturally explained by a large free energy of reaction, $\Delta G^{\ddagger}_{back} Z$, due to solvent reorganization.

3.5. 6HQc in Acetonitrile. We now turn to the transient spectra of 6HQc in acetonitrile shown in Figure 8. Recall that the fluorescence spectrum, its decay, and quantum yield in acidic acetonitrile correspond to the cation, indicating that the excited-state PT reaction does not occur (or is strongly suppressed) in these conditions. In spite of that, a clear fast evolution is observed during the first 5 ps. The C-band around 450 nm experiences a weak red-shift and decay, whereas a negative signal between 550 and 600 nm develops, similar to what is observed in water (Figures 4 and 5). Such behavior suggests that PT in fact takes place, although the equilibrium is strongly shifted to the reactant 6HQc. A biexponential fit of the growing Z-band (Figure 8c) shows that the signal develops again 2−3 times slower than solvent relaxation. Thus, in acidic acetonitrile, as in water, the reaction is solvation-controlled but proceeds with much smaller extension.

It has already been mentioned that spectroscopic-grade acetonitrile contains residual water at concentrations of 10^{-3}−10^{-2} M, as determined by the Karl−Fischer method. If we take into account the calculated energy, 47 kJ/mol, of hydrogen-bonding in the complex 6HQc:H_2O, then most of the cations should be bound to at least one water molecule. It is therefore reasonable to ascribe the spectral evolution in acetonitrile (Figure 8) to a relaxation process in photoexcited 6HQc:H_2O.

3.6. 6HQc in Acetonitrile−Water Solution. The spectral evolution of 6HQc in water−acetonitrile mixtures is similar to that in neat water, presented in Figure 4. However, the intensities of the C-band and Z-band depend now on water concentration. Figure 9a shows that the short-time PT signal (at $t = 5$ ps) increases in absolute value with growing water content. This

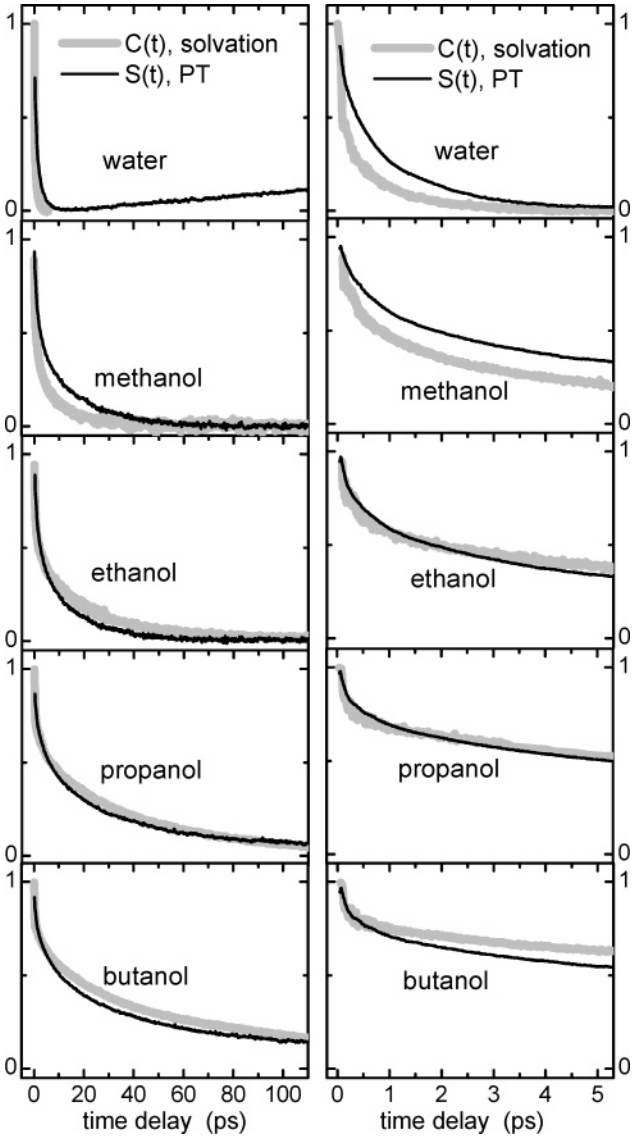

Figure 7. Comparison between the PT dynamics $S(t)$ (black curves) for 6HQc in protic solvents and the solvation dynamics $C(t)$ (gray). $C(t)$ was measured with 6MQz in water, methanol, and ethanol and with C153 in propanol and butanol. $S(t)$ closely follows $C(t)$, indicating that PT is solvation-controlled.

dependence can be qualitatively understood by assuming that PT takes place only for those 6HQc:H_2O complexes which have a sufficient amount of free water molecules in their surroundings. Then, with increasing water content, more cations acquire the proper surroundings, resulting in a growth of the zwitterion signal. The corresponding normalized PT kinetics $S(t)$ are presented in Figure 9b. Note that there is no water concentration dependence. It is evident that the evolution is solvation-controlled and that there is a gradual change from acetonitrile to water with increasing water content. The differences in PT kinetics are small, as expected from comparison of the corresponding solvation correlation functions, which are very close for these two solvents.

Considering the same evolution on a 100 ps time scale, displayed in Figure 10, one observes a long-time contribution to PT. This contribution manifests already in neat acetonitrile (with residual water) as a slow (∼1 ns) rise in the signal. For higher water concentrations the evolution becomes faster. We ascribe this long-time signal to diffusion-controlled PT which

(36) (a) Sumi, H.; Marcus, R. A. *J. Chem. Phys.* **1986**, *84*, 4894−4914. (b) Nadler, W.; Marcus, R. A. *J. Chem. Phys.* **1987**, *86*, 3906−3924.

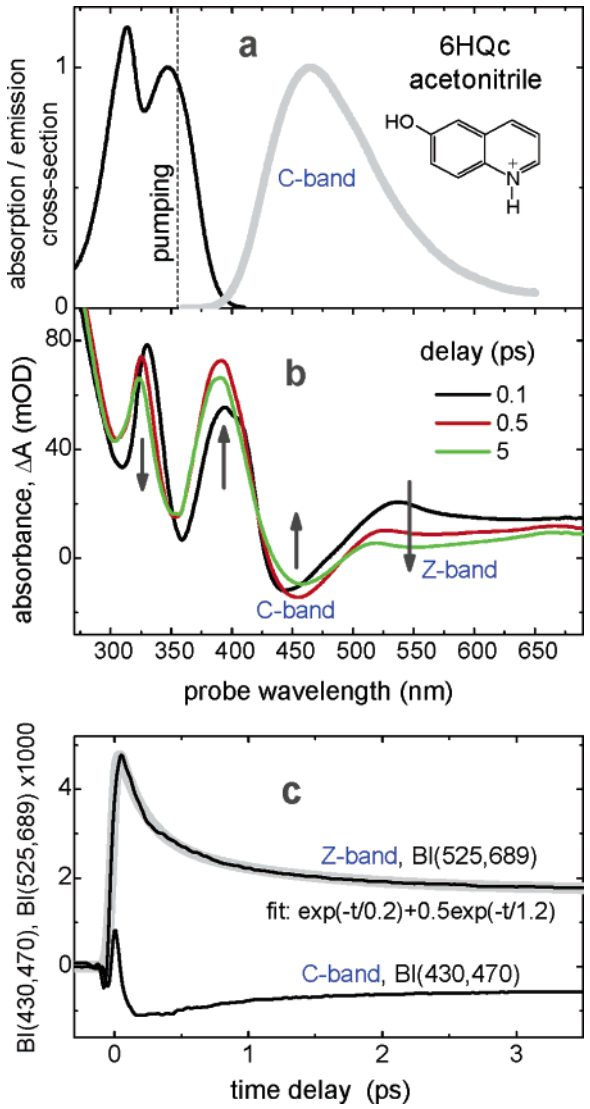

Figure 8. (a) Stationary absorption and stimulated emission spectra of 6HQc in acetonitrile. (b) Transient spectra of 6HQc in acetonitrile from 0.1 to 5 ps. A quasi-stationary spectrum at 5 ps (green) shows a red-shift and weak decay of the C-band. The PT reaction takes place but its equilibrium is strongly shifted to the cation. (c) The evolution of the C-band and Z-band. A fit (gray) shows that the reaction is 2−3 times slower than solvation (Table 2). Hence, PT is solvation-controlled, with a barrier of 2.5 kJ/mol, similar to PT in water.

originates from those cations which are initially *not* surrounded by water. Upon photoexcitation, water molecules diffuse to these cations, resulting in the long-time zwitterion signal. The diffusion rate can be obtained from three-exponential fits, $a_1 \exp(-t/\tau_1) + a_2 \exp(-t/\tau_2) + a_3 \exp(-t/\tau_3)$ (gray), of the experimental kinetics (black). In these fits $\tau_1 = 1.4$ ps was kept fixed, τ_3 was restricted around 1 ns, and only τ_2 was allowed to vary. The rate $1/\tau_1$ corresponds to the short-time solvation-controlled PT, and $1/\tau_2$ represents the diffusion contribution to PT. $1/\tau_3$ accounts for the fluorescence decay and is not well determined in our experiment. The dependence of the rate $1/\tau_2$ on water concentration is shown in Figure 11. The data are shown up to 15 M (at higher concentrations τ_2 approaches τ_1 and the two cannot be reliably separated). The best fit is linear and gives the proportionality coefficient $k_D = 10^{10}$ M^{-1} s^{-1}, which is very close to the rate of monomolecular diffusion in water or in

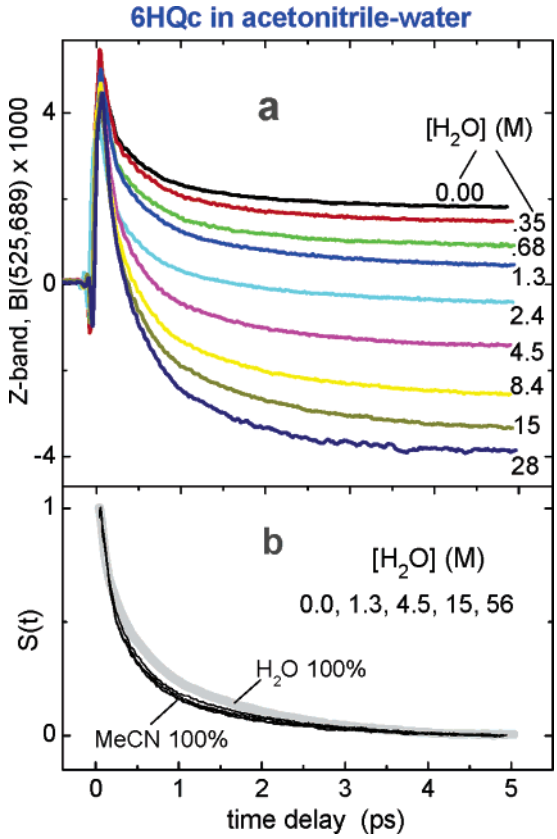

Figure 9. (a) Short-time evolution of the Z-band for 6HQc in acetonitrile−water solutions from the band integrals BI(525,689). The zwitterion signal at $t = 5$ ps increases with water concentration. This evolution reflects solvation-controlled PT from those cations which are surrounded by a sufficient number N of water molecules which can accept the photodetached proton. (b) The same normalized signals $S(t)$ reveal that the reaction is controlled by solvation in acetonitrile for low water concentrations (black curves) and by solvation in water for a high water content.

acetonitrile.[37] This indicates[1,11,38] that diffusion of only *one* bulk water molecule to a complex 6HQc:H_2O is sufficient to initiate the PT reaction.

This picture can be further verified by examining the concentration dependence of the short-time zwitterion signal in Figure 9a. Let us assume a Poisson distribution, $p(N) = \langle N\rangle^N e^{-\langle N\rangle}/N!$, of N bulk-water molecules around the solute ($\langle N\rangle$ is the average number or concentration of these molecules). We also assume that $(N + 1)$ water molecules are necessary for the "instantaneous" reaction. Then, the short-time signal should be proportional to the integral probability $P(N|\langle N\rangle)$ for having $(N + 1)$ or more surrounding molecules:

$$P(N|\langle N\rangle) = 1 - \sum_{j=0}^{N} \frac{\langle N\rangle^N \exp(-\langle N\rangle)}{N!} \qquad (6)$$

where N has to be determined by comparison with experiment. Figure 12a shows the distribution $P(N|\langle N\rangle)$ as a function of $\langle N\rangle$ for various values of N. The experimental PT signal (symbols) is shown in Figure 12b. The best fit is achieved for $N > 0$ (which means $N \geq 1$) and confirms that enrichment of the nearest

(37) Caldin, E. F. *The mechanism of fast reaction in solution*; IOS Press: Burke, VA, 2001; p 17.
(38) Solntsev, K. M.; Huppert, D.; Agmon, N.; Tolbert, L. M. *J. Phys. Chem. A* **2000**, *104*, 4658−4669.

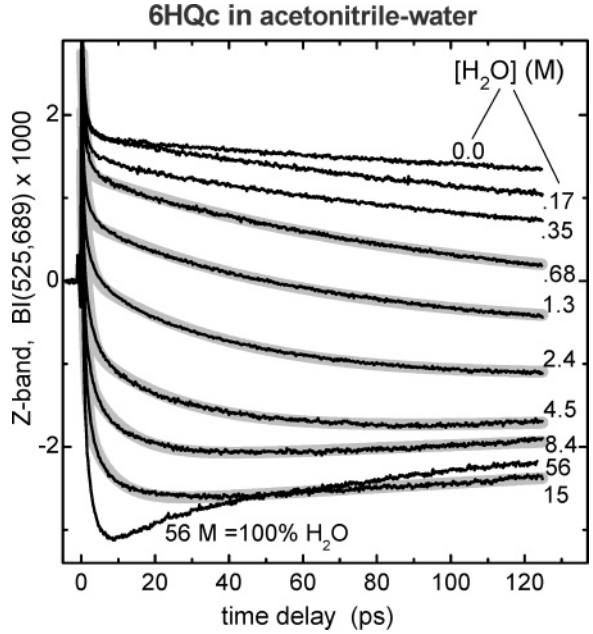

Figure 10. Long-time evolution of the Z-band for 6HQc in acetonitrile−water mixtures (black curves), showing a diffusion contribution to the reaction on a 10 ps to 1 ns time scale. The reaction rate increases with water concentration, as expected for diffusion. Gray lines are three-exponential fits with $\tau_1 = 1.4$ ps kept fixed, τ_3 restricted around 1 ns, and only τ_2 allowed to vary. The reaction rates $1/\tau_2$ result in the diffusion rate $k_D = 10^{10}$ s^{-1} M^{-1} for water in acetonitrile (see Figure 11).

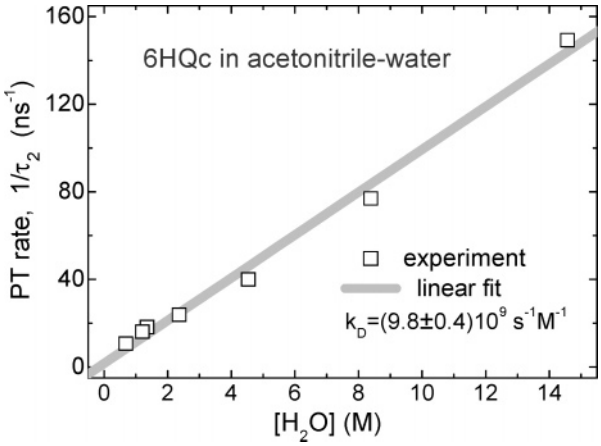

Figure 11. Reaction rate $1/\tau_2$ (symbols) for PT from 6HQc to acetonitrile−water as a function of water concentration, derived from the three-exponential fits in Figure 10. The slope of a linear fit (gray) gives the diffusion rate $k_D = 9.8 \times 10^9$ s^{-1} M^{-1}, consistent with a simple diffusion model.

solvent neighbors of the cation by only *one* water molecule is sufficient to initiate the PT reaction.

The next question is, how many water molecules are necessary to accept the photodetached proton? From the previous discussion of the dominant cationic form 6HQc:H_2O, the answer is apparently *two*, and the relevant structure is 6HQc:H_2O:H_2O. It is this form which can provide the necessary condition for the ultrafast solvation-controlled component of PT in water−acetonitrile mixtures. Only those cations which pre-exist in such form before photoexcitation are responsible for the short-time PT signal in Figures 9 and 12. The rest of the cations, in the form 6HQc:H_2O, cannot contribute to PT until they meet the second water molecule in the course of diffusion. It is reasonable to assume that PT proceeds through hydrogen bonds in two

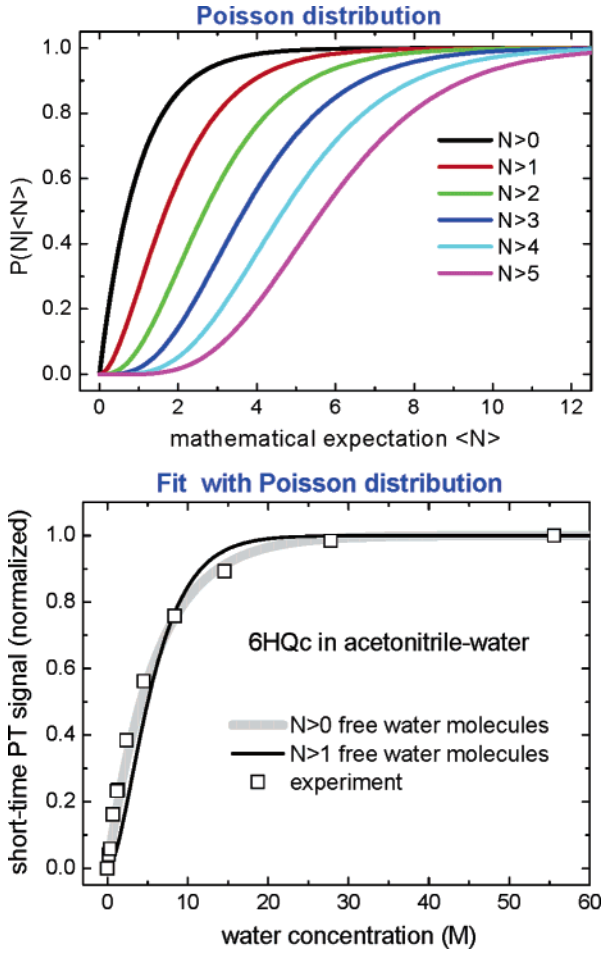

Figure 12. (Top) Integral Poisson distribution $P(N|\langle N\rangle)$ (see eq 5), showing that *more than N* molecules are involved, with $\langle N\rangle$ being the average (mathematical expectation). (Bottom) The short-time PT signal (symbols) from Figure 9a at $t = 5$ ps relative to neat acetonitrile. A fit to $P(N|\langle N\rangle)$ is obtained by scaling the graphs on the top along the *x*-axis. The best fit (gray) corresponds to $N > 0$ (that is, $N \geq 1$), indicating that only *one water molecule from the bulk* is sufficient to complete PT. The fit for $N > 1$ (thin black) is shown for comparison.

steps, from the cation to the nearest water molecule and then to the second one. Why is one water molecule not enough to complete PT? A possible explanation is that, in the intermediate 6HQz:H_3^+O, the zwitterion and proton are too close to each other to be effectively solvated. As a result, the equilibrium of the reaction 6HQc:$H_2O \rightleftarrows$ 6HQz:H_3^+O is strongly shifted to the cation (this is the case in acetonitrile).

4. Conclusions

We have studied PT to solvent from strong photoacids 6HQc and 6MQc in water, alcohols, and acetonitrile−water mixtures. In neat protic solvents the reaction is solvation-controlled, with a low barrier of ~2 kJ/mol. $C(t)$ is the true reaction coordinate; other processes such as intrinsic (microscopic) PT are faster than solvation and hence take place on a 10 fs or shorter time scale.

Upon photodissociation, no intramolecular ET occurs in the zwitterions 6MQz or 6HQz on a subpicosecond or longer time scale. This conclusion follows from our measurements on 6MQz. The assumption of "coupled proton and electron transfer" was introduced to explain the absence of the back-PT reaction.

However, our results show that back-PT is suppressed because of solvent stabilization.

In acetonitrile−water mixtures, PT proceeds on two distinctly different time scales. The fast solvation-controlled PT occurs for those photoacids which have a proper water surrounding, namely a sufficient number of water molecules in the vicinity of the cation. The slow diffusion contribution to PT comes from the rest of the excited cations which, during their lifetime, acquire water molecules in their surroundings due to diffusion. We were able to establish that only *one water molecule from the bulk* is necessary to initiate the photoreaction.

The cation in water can be present in two forms, 6HQc and 6HQc:H_2O. Our calculations favor 6HQc:H_2O, since the hydrogen-bonding between 6HQc and H_2O (47 kJ/mol) is 4 times more intense than that between two water molecules. Therefore, even in "neat" acetonitrile, the cation should be in the form 6HQc:H_2O because of residual water impurities. Consequently, at least two water molecules are necessary to accept the photodetached proton. Subsequent solvation of the proton and of the zwitterion completes the PT reaction.

We propose that the ultrafast solvation-controlled PT proceeds through the hydrogen bonds as

$$6HQc{:}H_2O{:}H_2O \rightleftarrows 6HQz{:}H_3{}^+O{:}H_2O \rightleftarrows 6HQz{:}H_2O{:}H_3{}^+O \quad (7a)$$

where each step is controlled by solvation. The diffusion contribution in water−acetonitrile mixtures is accounted for by

$$6HQc{:}H_2O + H_2O \rightleftarrows 6HQc{:}H_2O{:}H_2O \quad (7b)$$

and afterward the reaction proceeds according to (7a). In acetonitrile with residual water, only the first step of (7a) would take place:

$$6HQc{:}H_2O \rightleftarrows 6HQz{:}H_3{}^+O \quad (7c)$$

In this sense the product in acetonitrile can be considered as the reaction intermediate in protic solvents and mixtures. However, the PT equilibrium between the cation and the intermediate is strongly shifted to the reactant. A reason for this is probably that, in the complex 6HQz:$H_3{}^+O$, the proton and zwitterion are too close to each other to be effectively solvated.

Future experiments in extra-dry solvents are necessary to confirm our assumption of the dominant form 6HQc:H_2O. Also of interest are experiments in water−dioxane mixtures to scan the polarity dependence, measurements extended to 10 ns, and temperature-dependent measurements.

Acknowledgment. Financial support from the Deutsche Forschungsgemeinschaft through SFB 450, from the Spanish Ministerio de Educación y Ciencia (Project CTQ2004-07683-C02-01/BQU), and from the Xunta de Galicia is gratefully acknowledged. We also pleased to acknowledge the group of Tim Clark at the Computer Chemie Centrum (CCC, University of Erlangen-Nürnberg, Germany) and the CESGA (University of Santiago de Compostela, Spain) for sharing with us their computational facilities. S.A.K. thanks the Xunta de Galicia for the possibility to visit the University of Santiago in 2004−2005.

Supporting Information Available: Complete ref 26. This material is available free of charge via the Internet at http://pubs.acs.org.

JA0664990